



Trade Science Inc.

Materials Science

An Indian Journal

Full Paper

MSAIJ, 5(2), 2009 [77-84]

Influence of a preliminary aging treatment on the kinetic of oxidation at high temperature for a nickel-based alloy reinforced by chromium carbides

Patrice Berthod

Laboratoire de Chimie du Solide Minéral (UMR 7555), Faculté des Sciences et Techniques,
UHP Nancy 1, Nancy-Université, B.P. 239, 54506 Vandoeuvre-lès-Nancy, (FRANCE)

E-mail : Patrice.Berthod@lcsm.uhp-nancy.fr

Received: 7th December, 2008 ; Accepted: 12th December, 2008

ABSTRACT

The aim of this work is to examine if the modified morphology of interdendritic carbides coarsened by an initial aging treatment can lead to a modified behaviour of the alloy in oxidation at high temperature. This was done here with a model Ni-30Cr-1.0C cast alloy which was first exposed to 1200°C for 5, 25 or 100 hours. Samples cut in the middle of the alloy were thereafter subjected to oxidation by air at 1000, 1100 and 1200°C for 50 hours. The thermogravimetry results were treated in order to specify the rates of transient oxidation, of parabolic oxidation and of chromia volatilization (according to the law $m \times dm/dt = K_p - K_v x_m$), and finally of oxide spallation at cooling. The corresponding constants K_p , K_p and K_v were determined in all cases and they showed that oxidation rate and chromia volatilization rate increase with the preliminary aging duration while, in contrast, oxide spallation at cooling is delayed down to lower temperatures.

© 2009 Trade Science Inc. - INDIA

KEYWORDS

Nickel alloy;
Chromium carbides;
Aging;
High temperature oxidation;
Oxide spallation.

INTRODUCTION

After a long time spent at very high temperature, the microstructure of superalloys may have significantly evolved, under applied stress or not. As examples one may evocate the coarsening of grains or of carbides^[1], the rafting structure appeared in γ/γ' nickel-based superalloys^[2], the fragmentation of the tantalum carbides fibres in the CoTaC *in situ* composite directionally solidified Co-based superalloys^[3] or of interdendritic eutectic MC-carbides in cobalt-based alloys^[4,5] as well as in nickel and/or iron-based alloys^[6]. These microstructure changes generally induce mechanical

weakness for the alloys, but they may also modify their resistance against oxidation, especially in the case of transformation of interdendritic chromium-containing carbides. Indeed, it is well known that, on the one hand such carbides play as chromium suppliers, and on the other hand grain boundaries are privileged diffusion paths for chromium^[7].

The purpose of this study is to observe if a more or less long aging treatment initially applied to a simple ternary nickel-based alloy can significantly modify the high temperature oxidation behaviour by changing both morphology and volume fraction of its interdendritic network of chromium carbides.

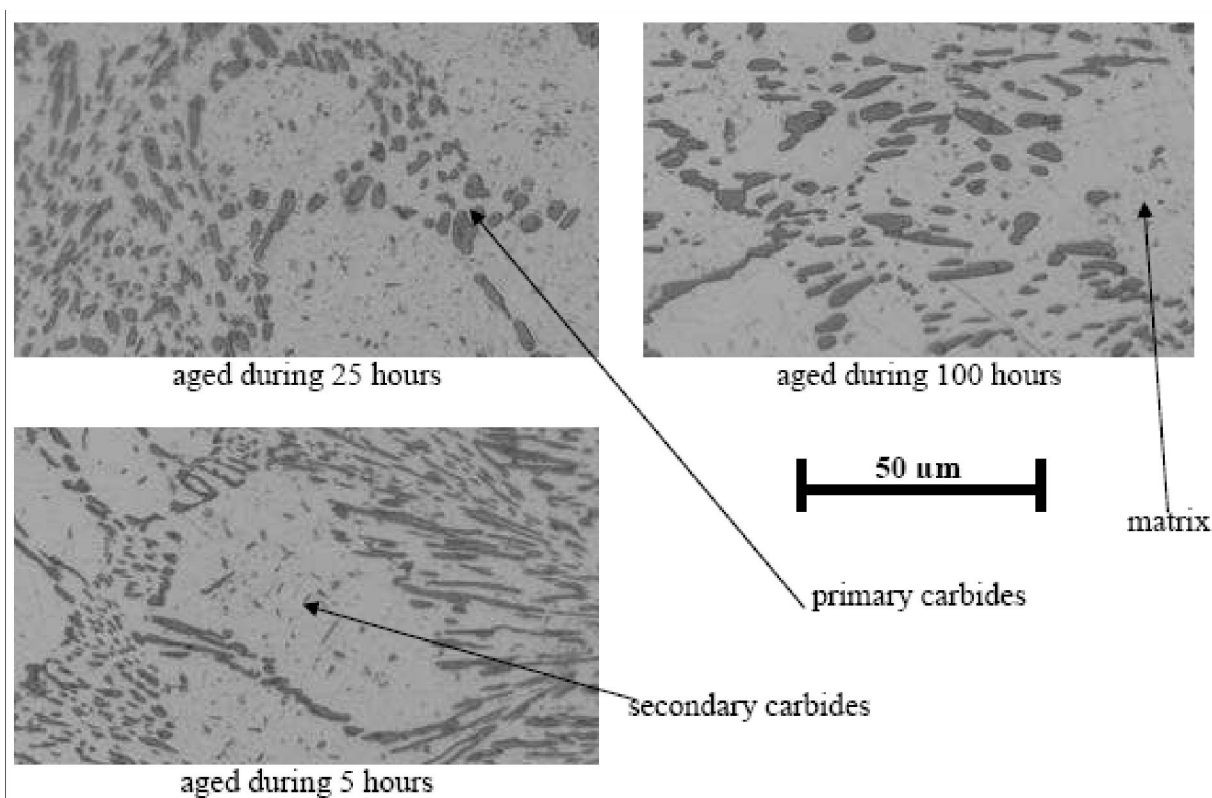


Figure 1 : Microstructures of the studied alloys after the three aging treatments (Grosbeck etching)

EXPERIMENTAL

The studied alloys

The alloys which were involved in this study are the same ones which were studied in a recent work^[8] concerning the effect of aging treatment on the thermodilatometry behaviour. It can be remembered that these alloys were elaborated by foundry from pure elements (purity > 99.9%) melted with a high frequency induction furnace. Three ingots, all of them of about 100g, were obtained and were heat-treated at 1200°C for three different durations (before air quenching): the first one for 5 hours, the second one for 25 hours and the last one for 100 hours. The three ingots were then cut in order to get a first part for chemical composition analysis (which led to a same composition of Ni(bal.)-30±1wt.%Cr-1wt.%C) for the three ingots) and microstructure examination (figure 1, optical micrograph after etching for 1min with Grosbeck solution). One also prepared three others parts per ingot (parallelepipeds of about 7×7×3mm³), by cutting then polishing the main faces and smoothing the edges with

1200 grit paper, to obtain samples ready for oxidation tests with continuous mass gain recording.

Thermogravimetry runs and metallographic examinations

Three parallelepiped samples per ingot (i.e. per heat treatment) underwent oxidation tests. They were performed at 1000, 1100 and 1200°C using a Setaram thermobalance (type: TAG 1750 Simultaneous symmetrical thermoanalyser) under a dry industrial air flow (80%N₂, 20%O₂) at 1 L h⁻¹. Preliminary heating (respectively final cooling) was realized at 20 K min⁻¹ (resp. -10 K min⁻¹), and the dwell duration was 50 hours, for all tests. Temperature and mass gain values were recorded every 40 seconds. After test, the oxidized samples were embedded in a cold {resin + hardener} mixture, polished with grinding papers from 240 grit to 1200 grit. After ultrasonic cleaning, they were mirror-like polished with 1μm alumina suspension, then etched at room temperature by immersion in a Grosbeck solution (4g NaOH and 4g KMnO₄ in 100mL of distilled water) for about 1 minute, in order to reveal the chromium carbides. Metallographic

examinations were done using a metallographic optical microscope (Olympus, type: Vanox-T) equipped with a DP-11 camera for taking jpeg pictures.

Mathematical treatment of the mass gain results: transient oxidation

Generally, during the preliminary heating, oxidation starts affecting the samples when temperature is become high enough. This first part of transient oxidation is followed, at the beginning of the isothermal dwell, by a second part which is of the $\{dm=K_1 \times dt\}$ -type, where m is the mass gain per surface unit (in $g\ cm^{-2}$) and K_1 is a linear kinetic constant (in $g\ cm^{-2}\ s^{-1}$), until the Wagner's^[9] parabolic oxidation is established. Thus, the exploitation of each file of thermogravimetric measurements began with the determination of the linear constant K_1 . Knowing these K_1 values for 1000, 1100 and 1200°C, it was checked that this linear constant really obeys an Arrhenius law, which allowed thereafter assessing the mass gain obtained during the whole heating before the dwell (this procedure was extensively described in a previous study^[10]). This mass gain obtained during the heating phase was added to the isothermal mass gain obtained during the second part of the transient oxidation to know the initial mass gain m_0 existing just before the parabolic oxidation starts.

Mathematical treatment of the mass gain results: parabolic oxidation and chromia volatilization

The thermogravimetric results were analysed in order to assess with accuracy the parabolic rate by taking into account the partial volatilization of the external chromia which forms almost exclusively all around the sample surface. Indeed, when temperature is higher than 1000°C, this protective stoichiometric $Cr^{III}_2O_3$ oxide can be re-oxidized into a new oxide $Cr^{VI}O_3$ which is gaseous at such temperature, and it is important to calculate the corresponding loss in mass in order to avoid minimizing the kinetic of parabolic oxidation.

This was done by treating the mass gain files by considering the equation {Eq.1}, in which the volatilization of chromia is proportional to the elementary time step dt through the expression $-K_v \times dt$ where K_v is the volatilization constant. This equation can also be rewritten {Eq.2} to express the mass gain m multiplied by its own derived function dm/dt , as a linear function

of m itself.

$$dm = \frac{K_p}{m} \times dt - K_v \times dt \quad (1)$$

$$m \times \frac{dm}{dt} = K_p - K_v \times m \quad (2)$$

with m expressed in $g\ cm^{-2}$, K_p (Wagner's parabolic constant) in $g^2\ cm^{-4}\ s^{-1}$ and K_v (chromia volatilization constant) in $g\ cm^{-2}\ s^{-1}$.

Thereafter, plotting $m \times dm/dt$ versus $-m$ leads to a straight line, characterized by an ordinate at the origin equal to K_p and by a slope equal to K_v , leading easily to the values of both K_p and K_v ^[10]. Unfortunately, in

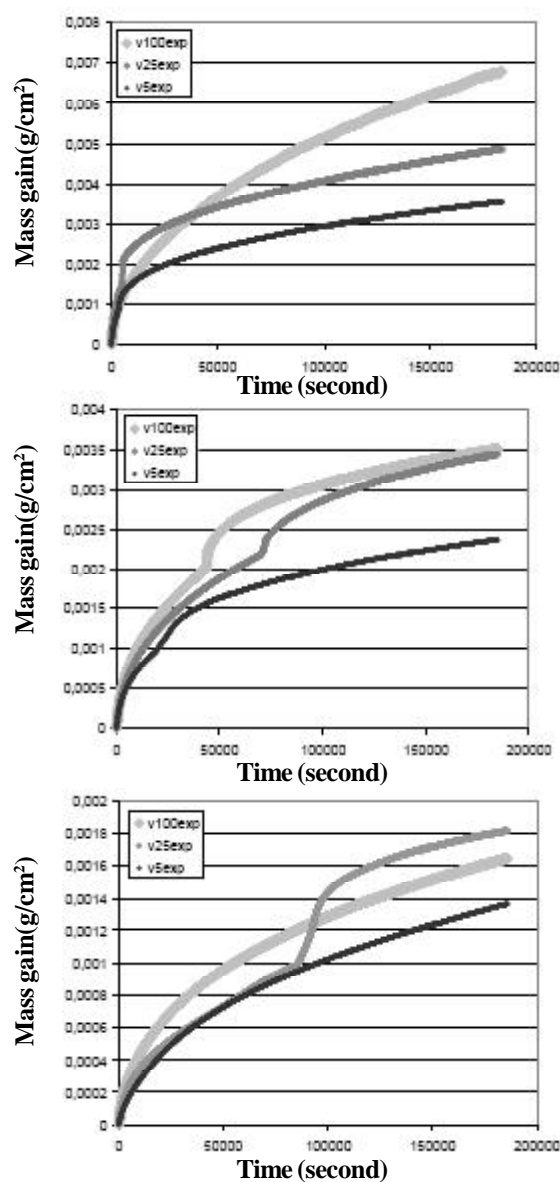


Figure 2 : Mass gain curves for the three aging treatments, for 1200°C (top), 1100°C (middle) and 1000°C (bottom)

Full Paper

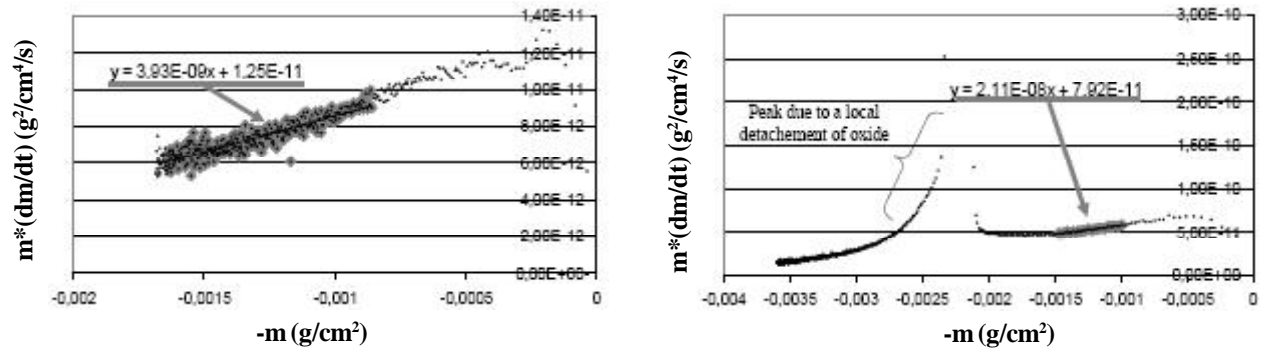


Figure 3: Examples of numerical treatment of the data: 100h-aged alloy oxidized at 1000°C (left) and at 1100°C (right)

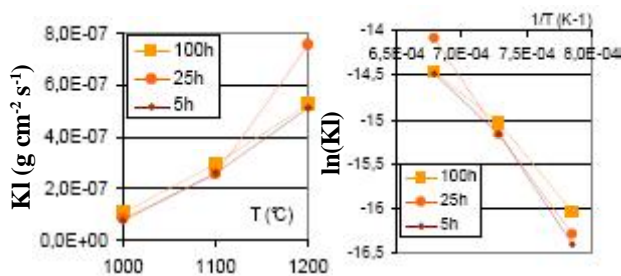


Figure 4: The linear K_1 constant plotted versus temperature linearly (left) and according to the Arrhenius representation (right)

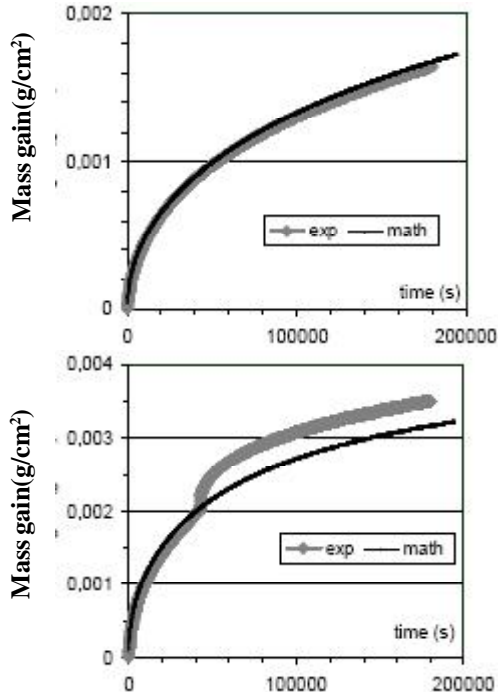


Figure 5: Experimental curves and corresponding mathematical curves rebuilt with the deduced values of K_p and K_v : 100h-aged alloy oxidized at 1000°C (top) and at 1100°C (bottom)

practice the small lack of precision of thermobalances is responsible of dispersion of the values of the derived term dm/dt , and then of $m \times dm/dt$; the values of dm/dt must be estimated by the regression coefficient calculated from eleven successive couples (t , m) surrounding the considered time (from which a new time step equal to ten times the initial measure time step).

Characterization of oxide spallation during final cooling

The modifications induced by a preliminary aging treatment may also have some consequences for the adherence of the external oxide on the alloy surface, and also for the shear stresses developing at the oxide-alloy interface at cooling since the thermodynamic behaviour of the alloy can be slightly changed because of this aging treatment^[8]. Thus, the mass evolution at cooling was also examined during the post-test cooling, following a similar procedure as previously presented^[11,12].

RESULTS AND DISCUSSION

The obtained thermogravimetry curves

The curves plotting the mass gain versus time are all almost of the parabolic type (figure 2), even if local oxide detachments due to internal compressive stresses increasing in oxide during its thickening occurred in some cases. These jumps of mass gain in these curves were responsible of the corresponding peaks sometimes observed on the values of $m \times dm/dt$ plotted versus $-m$ (examples in figure 3), but they did not represent a problem for the analysis of the curves according to equation {Eq.2}. One can first remark that the duration of the aging treatment seems having a real effect on the

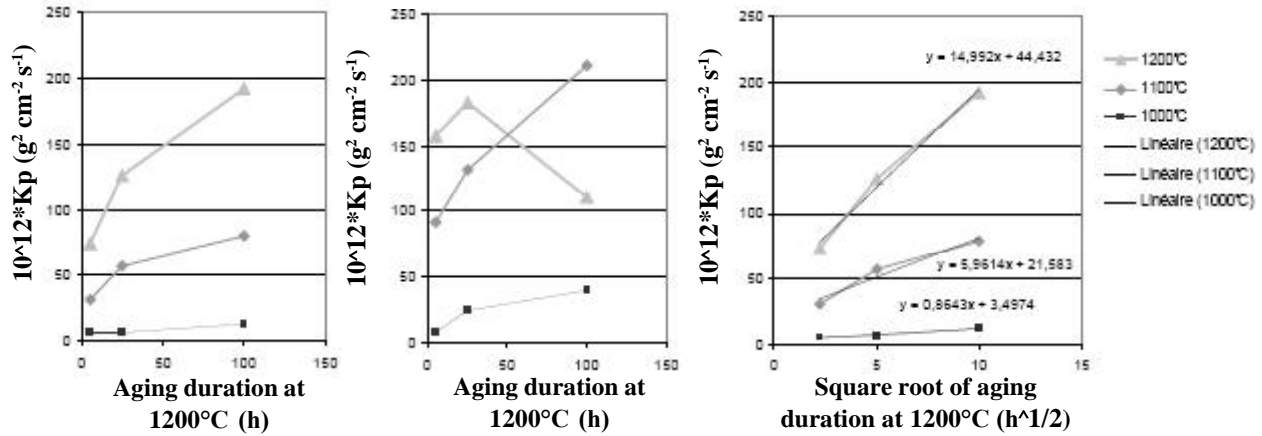


Figure 6: Variation of K_p (left hand) and of K_v (middle) versus the aging duration; right hand: variation of K_p versus the square root of aging duration

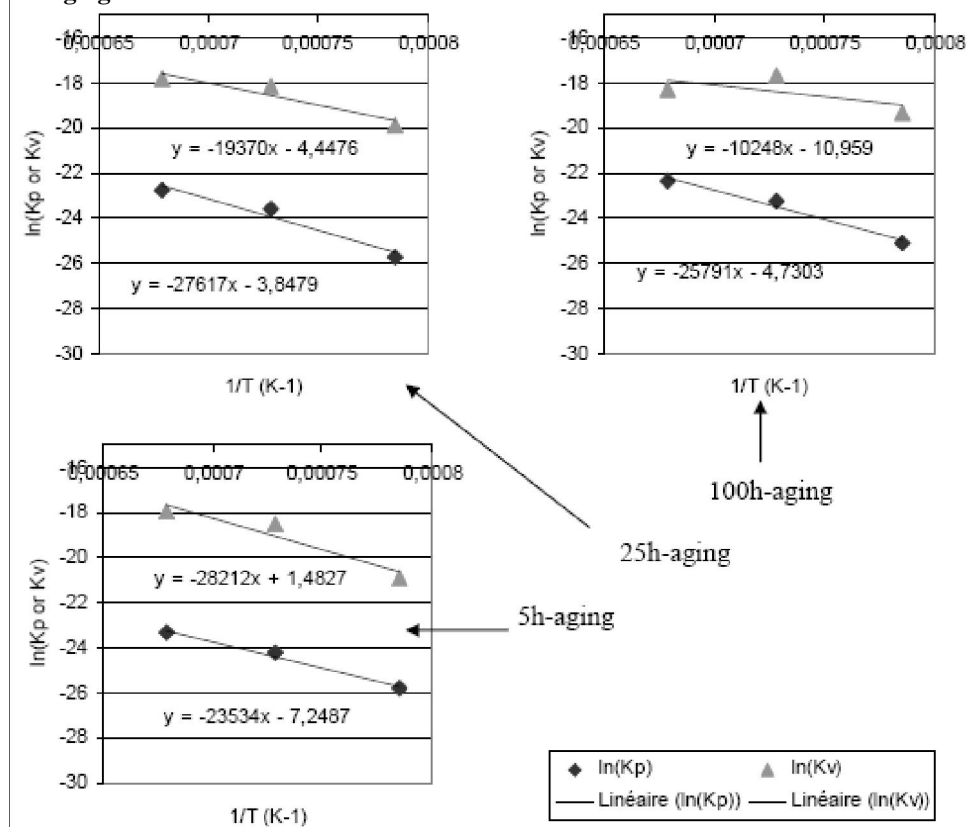


Figure 7: Arrhenius plot for the parabolic constant and the volatilization constant for the three aging treatments

mass gain kinetic whatever the temperature of oxidation test since globally the curves corresponding to a 100h-aging are above the ones for a 25h-aging, and the latter are themselves above the curves for a 5h-aging.

The linear constants of transient oxidation

The linear constants tend to follow the same order as the global mass gain curve (figure 4, left hand), but less systematically (example: oxidation test at 1200°C

on an alloy aged during 25h). K_1 globally obeys an Arrhenius law (figure 4, right hand): the activation energies are 150, 171 and 124 kJ mol⁻¹, for aging durations equal respectively to 5h, 25h and 100h.

The parabolic constants and chromia–volatilization constants

The simultaneous determination of the kinetic constant K_p describing the parabolic oxidation related

Full Paper

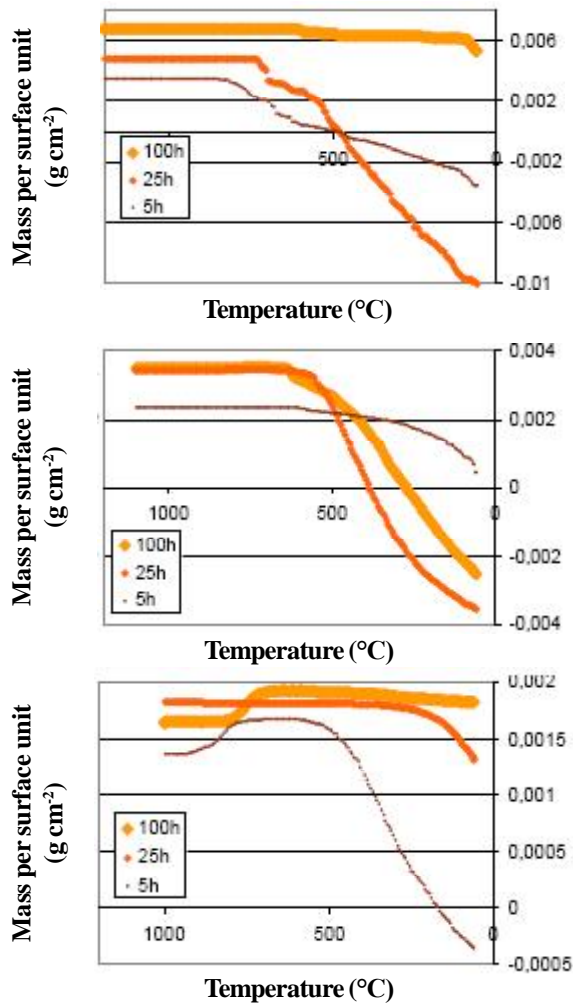


Figure 8: Progress of mass loss at cooling because of oxide spallation: after 50h of oxidation at 1200°C (top), 1100°C (middle) and 1000°C (bottom)

to the Wagner's law^[9] and of the kinetic constant K_v characterizing the rate of chromia volatilization was achieved in good conditions in all cases and the values obtained for K_p and K_v , used for rebuilding mathematical curves step by step according to {Eq.3}, allowed verifying that these artificial curves are well superposed with the experimental curves or, at least, are well parallel to them (figure 5).

$$m_{n+1} = m_n + \delta m_{n+1} = m_n + \frac{K_p}{m_n} \times \delta t - K_v \times \delta t \quad (3)$$

in which m_n and m_{n+1} are the values of the mass gain at respectively $t_n = n \times \delta t$ and $t_{n+1} = t_n + \delta t = (n+1) \times \delta t$ with $\delta t = 400s$ (new time step), K_p and K_v are the values issued from the treatment of the experimental curves.

The values are given in figure 6, plotted versus the

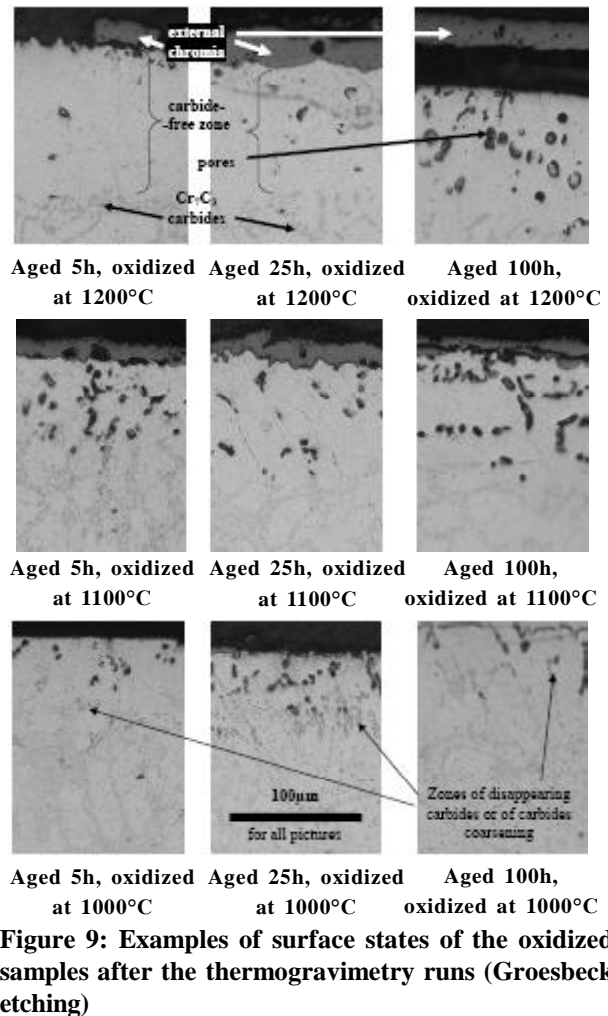


Figure 9: Examples of surface states of the oxidized samples after the thermogravimetry runs (Groesbeck etching)

duration of the preliminary aging treatment or versus the square root of this duration, while the values of their neperian logarithms are plotted versus the reciprocal temperature in figure 7 (i.e. in representation of Arrhenius).

The parabolic constant K_p , which is naturally higher when temperature is higher, also increases when the aging duration increases, seemingly following a parabolic law versus this duration of the preliminary aging treatment. This interesting observation is almost confirmed by plotting the value of K_p versus the square root of the aging duration. Furthermore it should be possible to propose values of the multiplying factor (another "parabolic" constant ...): $15 \times 10^{-12} \text{ g}^2 \text{ cm}^{-4} \text{ s}^{-1} \text{ h}^{-1/2}$ (or $0.25 \times 10^{-12} \text{ g}^2 \text{ cm}^{-4} \text{ s}^{-3/2}$), $6 \times 10^{-12} \text{ g}^2 \text{ cm}^{-4} \text{ s}^{-1} \text{ h}^{-1/2}$ (or $0.1 \times 10^{-12} \text{ g}^2 \text{ cm}^{-4} \text{ s}^{-3/2}$) and $0.9 \times 10^{-12} \text{ g}^2 \text{ cm}^{-4} \text{ s}^{-1} \text{ h}^{-1/2}$ (or $0.015 \times 10^{-12} \text{ g}^2 \text{ cm}^{-4} \text{ s}^{-3/2}$), for 1200, 1100 and 1000°C respectively.

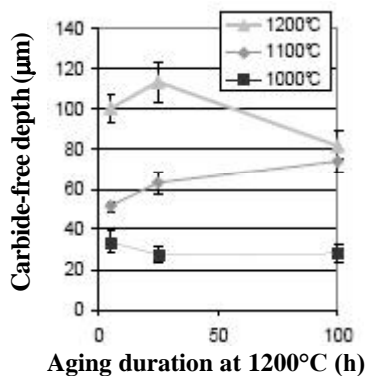


Figure 10: Average (\pm standard deviation) depth of the carbide-free zone plotted versus the duration of the 1200°C-aging treatment

One can observe a similar dependence of the volatilization constant K_v on the temperature of oxidation test, and also on the duration of the aging treatment, except in the case of the K_v obtained at 1200°C for the alloy with the longest aging duration (for which the volatilization constant is of the same order of magnitude as for 1100°C).

When analysed by plotting $\ln(K_p)$ and $\ln(K_v)$ versus the inverse value of the absolute temperature, the dependence of the constant on temperature is clearly of an Arrhenius type (figure 7). The activation energies for K_p are 196, 229, 214 kJ mol⁻¹ for an aging duration of respectively 5 hours, 25 hours and 100 hours. For K_v , the values are 235, 157 and 85* kJ mol⁻¹, for respectively 5h, 25h and 100h of aging duration (*: the curious value at 1200°C being also considered).

The progress of oxide spallation during cooling after isothermal oxidation

During the isothermal oxidation the increasing internal compression due to growth stresses inside the thickening oxide already caused local detachments from the substrate, as revealed by jumps in the mass gain curves (more at the two lowest temperatures than at 1200°C). When cooling starts at the end of the isothermal dwell, the thermal contraction of the alloy, which is more pronounced than the external oxide one due to the difference of thermal expansion coefficient between the two (about $20 \times 10^{-6} \text{ K}^{-1}$ for the alloy^[8] and $10 \times 10^{-6} \text{ K}^{-1}$ for chromia^[13]), enhances compression in the oxide. Then after a small time of cooling a local detachment can occur without breakdown, which allows

a new quick oxidation of the denuded part of the alloy (figure 8) before a real breakdown inducing a more or less rapid mass loss (figure 8), as encountered exclusively after isothermal oxidation at 1000°C. After oxidation at 1100 and 1200°C, the external oxide was obviously thick enough to resist detachment in the first part of cooling, but more or less fast (but continuous) mass loss finished to appear before the end of cooling. It can be noted that the temperature at which this mass loss began tends to be lower, and then the temperature difference between dwell and the spallation's beginning more important, when the preliminary aging treatment was longer. This is obvious for the cooling after isothermal oxidation at 1200°C (figure 8, top) and at 1000°C (figure 8, bottom), while spallation began after almost the same decrease in temperature from 1100°C for the three durations of preliminary aging (figure 8, middle).

The surface states of the oxidized samples

The optical micrographs presented in figure 9 illustrate the surface and sub-surface deterioration due to oxidation at high temperature. In all cases the external oxide (chromia) was lost, partly or entirely, during cooling, when exiting the thermobalance and/or during the metallographic preparation. Nevertheless, some parts remained on surface and can be observed. From the substrate surface (interface between oxide and alloy), there is first a zone in which carbides initially present have disappeared (with appearance of holes in some cases). This carbide-free zone, which was growing inwards during isothermal oxidation because of the diffusion towards the oxidation front of the chromium released by the dissolving carbides, is deeper when temperature of oxidation was higher, but its depth does not seem depending on the aging duration (figure 10).

General commentaries

Applying a preliminary aging treatment may influence the high temperature oxidation behaviour of alloys. This was observed here on a simple Ni-Cr-C alloy, first about the transient oxidation which tended to be faster, and second also about the parabolic oxidation for which a long duration of aging at 1200°C before test obviously led to greater mass gains at all times and to higher parabolic constants (which moreover increased with the

Full Paper

square root of aging duration). This tendency seemed to exist also for the rate of chromia volatilization, except one case-the 100h-aged alloy oxidizing at 1200°C- for which it is possible that an external NiO oxide partly protected the growing chromia from volatilization. Indeed, such an outer NiO scale can exist when nickel-based alloys oxidize at high temperature^[7,14], and this oxide was probably more present since the oxidation rate was especially high in this case (figure 2, top).

Unfortunately, the loss of the most part of the external oxide did not allow verifying that this oxide was especially present. When the values of K_v , but also of K_p and K_l are compared with others obtained with alloys of the same family (ternary Ni-30Cr-0 to 0.8C^[10,15]) it appears that there is globally a very good agreement for a same temperature. The values of volatilization constant are also of the same order of magnitude with older results^[16,17]. The sole mismatches that must be noted concern the volatilization constant of the Ni-30Cr-1.0C alloy of this study when it has been aged for 100 hours: K_v is often higher than what was measured with the same procedure for the Ni-30Cr-0 to 0.8C. In contrast, the linear, parabolic and volatilization constants of the Ni-30Cr-1.0C aged only for 5 hours are globally very close to the corresponding ones of the Ni-30Cr0.8C alloy^[15] at the same temperatures.

Even for the oxide spallation during cooling the 1200°C-aging duration seemed having an effect: the mass loss due to spallation generally began later for the most aged alloy than for the others, maybe because of a thicker chromia scale more resistant to the compression induced by cooling.

CONCLUSION

High temperature aging obviously may induce thereafter changes in the behaviour of alloys in situation of oxidation at high temperature. This was seen here in the case of a Ni-30Cr-1.0C alloy which is a very simple one but also which represents the base of more complex Ni-based superalloys reinforced by carbides. A global slight (but however significant) acceleration of the mass gain rate was noted, for the transient oxidation as well as for the parabolic oxidation. This was also true for the volatilization of chromia. For the moment, these observations only concern nickel-based alloys

containing eutectic chromium carbides, but it can be interesting to study that later in the case of other bases (e.g. cobalt) and other types of carbides (e.g. TaC), in order to know if such results could be encountered again.

ACKNOWLEDGMENTS

Lionel Aranda and Cédric Heil are gratefully thanked for their technical contribution to this work.

REFERENCES

- [1] E.F.Bradley; 'Superalloys: A Technical Guide', ASM International; Metals Park, (1988).
- [2] C.T.Sims, W.C.Hagel; 'The Superalloys', John Wiley and Sons, New York, (1972).
- [3] J.F.Stohr; Ann.Chim., **5**, 226 (1980).
- [4] P.Berthod; Materials Science: An Indian Journal, **4(3)**, 185 (2008).
- [5] P.Berthod; Materials Science: An Indian Journal, **4(4)**, 290 (2008).
- [6] P.Berthod, Y.Hamini, C.Vébert; Materials Science: An Indian Journal, **4(4)**, 284 (2008).
- [7] P.Kofstad; 'High Temperature Corrosion', Elsevier applied science, London, (1988).
- [8] P.Berthod, C.Heil, P.Lemoine; Materials Science, An Indian Journal, in press.
- [9] C.Wagner; Z.Phys.Chem., **21**, 25 (1933).
- [10] P.Berthod; Oxidation of Metals, **64(3/4)**, 235 (2005).
- [11] P.Berthod, L.Aranda, P.Lemoine; Materials Science, An Indian Journal (accepted paper).
- [12] P.Berthod, L.Aranda, C.Vébert; Materials Science, An Indian Journal (accepted paper).
- [13] P.Shaffer; 'High-Temperature Materials N°1', Plenum Press, New York, (1964).
- [14] P.Berthod; Ann.Chim.Sci.Mat., **33(3)**, 247 (2008).
- [15] P.Berthod; Oxidation of Metals, **68**, 77 (2007).
- [16] W.C.Hagel; Trans.ASM, **56**, 583 (1963).
- [17] C.A.Stearns, F.J.Kolh, G.C.Fryburg; J.Electrochem. Soc., **121(7)**, 945 (1974).